# Localization of gamma-ray bursts using POLAR

**Estela Suarez-Garcia[*†], Daniel Haas[*†], Wojtek Hajdas[§], Giovanni Lamanna[‡], Catherine Lechanoine-Leluc[*], Radosław Marcinkowski[¶], Aliko Mtchedlishvili[§], Silvio Orsi[*], Martin Pohl[*], Nicolas Produit[†], Divic Rapin[*], Dominik Rybka[¶], and Jean-Pierre Vialle[‡]**

[*]*DPNC, 24 Quai Ernest-Ansermet, Université de Genève, 1205 Genève, Switzerland.*
[†]*INTEGRAL Science Data Centre, 16 Chemin d'Écogia, 1290 Versoix, Switzerland*
[‡]*LAPP, Université de Savoie, CNRS/IN2P3, Annecy-le-Vieux, France*
[§]*Paul Scherrer Institut, 5232 Villigen PSI, Switzerland*
[¶]*The Andrzej Soltan Institute for Nuclear Studies, 69 Hoza str., 00-681 Warsaw, Poland*

***Abstract*. POLAR is a compact instrument devoted to measure the linear polarization of the gamma-ray bursts (GRBs) prompt emission. The position of the detected GRB with respect to the POLAR coordinates is needed to determine its level of polarization. Using dedicated GEANT4 simulations we have developed a method by which, despite of the polarimeter incapability of taking images, GRBs can be roughly localized using POLAR alone. For this purpose scalers are attached to the output of the 25 multi-anode photomultipliers (MAPMs) that collect the light from the POLAR scintillator target. Simulations show that the relative outputs of the 25 scalers depend on the GRB position. A database of very strong GRBs simulated at 10201 positions has been produced. When a GRB is detected, its location is calculated searching the minimum of the $\chi^2$ obtained in the comparison between the measured scaler pattern and the database. This GRB localization technique brings enough accuracy so that the error transmitted to the 100% modulation factor is kept below 10% for GRBs with fluence $\mathrm{F_{tot}} \geq 10^{-5}$ erg cm$^{-2}$. The POLAR localization capability will be useful for those cases where no other instruments are simultaneously observing the same field of view.**

***Keywords*: Gamma-ray burst; source localization; POLAR**

## I. Introduction

Gamma-ray bursts (GRBs) are short flashes of $\gamma$-rays appearing at random positions in the sky, and considered to be the most violent explosions in the Universe. Their prompt emission presents a great variability of lightcurves and its spectrum follows a broken power law function, often described using the Band model [1]:

$$f(E) = A \begin{cases} \left(\frac{E}{100}\right)^{\alpha} & \exp\left(-\frac{E(2+\alpha)}{E_{\mathrm{peak}}}\right) \\ & \text{for} \quad E \leq (\alpha-\beta)\,\frac{E_{\mathrm{peak}}}{2+\alpha}, \\ \left(\frac{E}{100}\right)^{\beta} & \exp\left(\beta-\alpha\right)\left[\frac{(\alpha-\beta)E_{\mathrm{peak}}}{100(2+\alpha)}\right]^{(\alpha-\beta)} \\ & \text{for} \quad E \geq (\alpha-\beta)\,\frac{E_{\mathrm{peak}}}{2+\alpha} \end{cases} \tag{1}$$

The Band model fits the spectrum using four parameters: an amplitude ($A$), the low- and high-energy spectral indexes ($\alpha$ and $\beta$, respectively), and the peak energy ($\mathrm{E_{peak}}$) of the power density spectrum $\nu F_\nu$, which represents the total energy flux per energy band.

Precise polarimetry measurements of the GRB prompt emission can distinguish between different theoretical models, offering unique information on the emission mechanism of the GRBs and on the composition and geometric structure of their jets [2], [3]. To date, only a few measurements of the prompt GRB polarization have been performed, all of them with instruments that had not been designed for this purpose and lacked in many cases a good characterization of their systematic effects, enough effective area, or good background rejection mechanisms for polarimetry. In view of the power and the lack of precise polarization studies of GRBs, several X- and $\gamma$-ray polarimeters have been proposed and are under development. Some examples are POLAR [5], GRAPE (Gamma-Ray Polarimeter Experiment [6]), POET (Polarimeters for Energetic Transients, [7]), CIPHER (Coded Imager and Polarimeter for High Energy Radiation, [8]), PHENEX (Polarimetry for High ENErgy X rays, [9]), XPOL [10] and POLARIX [11].

## II. POLAR Instrument

POLAR [5], see figure 1, is a small and compact instrument designed to determine the level of linear polarization of the 50 – 500 keV photons arriving from the prompt emission of GRBs. POLAR consists of a target divided into 25 modules, each consisting of 64 plastic scintillator bars, optically coupled to one multi-anode photomultiplier (MAPM), and its corresponding front-end electronics, all together enclosed in a thin carbon fiber socket. The whole target, together with the central computer, the power supplies and the rest of the electronics, is further enclosed in a container box and mounted onto a satellite. A flight opportunity for POLAR on the future Chinese Tian-Gong Space Station is currently under consideration.

Hard X-ray photons arriving from a GRB have a high probability of experiencing Compton scattering in the target, generating a signal in more than one channel.

If the $\gamma$-ray emission from the GRB is not polarized, the modulation curve, i.e. the azimuthal distribution of the ensemble of photons that scatter inside POLAR target, is flat. Otherwise it follows a sinusoidal curve whose amplitude is the so-called *modulation factor*, and whose phase indicates the angle of linear polarization of the GRB photons [12], [13]. The modulation factor ($\mu$), divided by the response of the detector to a 100% polarized flux ($\mu_{100}$), is the polarization level ($\Pi$) of the incoming photons: $\Pi = \mu/\mu_{100}$. This principle allows POLAR to measure the level of polarization of the prompt emission of GRBs.

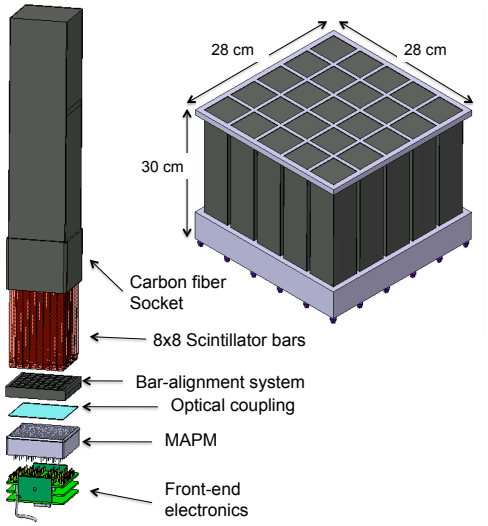


Fig. 1: Scheme of POLAR detector. *Left*: Exploded view of one module from POLAR target. *Right*: Complete POLAR target, i.e., the assembly of 25 modules, with its approximate dimensions.

An important part of the POLAR design and the evaluation of its polarimetric capabilities is performed using GEANT4 [14] simulations. The 1600 scintillator bars of the target have been simulated with their actual $6\times6\times200$ mm$^3$ dimensions and wrapped with a 50 $\mu$m thick aluminum foil. The target is further placed inside an aluminum box of 1 mm thickness that serves as a shield from low-energy charged particles and represents the outer enclosure of the detector. The incoming direction, the spectrum, and the type of particles to be used are generated following the user instructions. A specific routine has been developed to produce hard X-ray photons following the Band model spectrum [1] and its parameters. The standard physical processes that photons can undergo in the detector are taken into account, including polarized Compton scattering, photoelectric effect, and pair production, among others. The photon energy transfer into scintillation and the subsequent optical optical light collection processes have not been considered. The simulation generates a ROOT [15] file containing all the necessary data for the subsequent analysis: the incoming photon energy, the number and position of the bars fired, the energy deposited at each bar, etc.

Totally dedicated to polarimetry, the large field of view ($\sim$1/3 of the sky) of POLAR and its lack of imaging capability would in principle force the detector to rely on other instruments to provide the location of the observed GRBs. Such a limitation would reduce the number of GRBs to be measured by POLAR depending on whether another GRB detector would be observing the same portion of the sky or not. To minimize this drawback we have developed a method to roughly localize GRBs using only POLAR. For this purpose, scalers are to be attached to the output of the 25 MAPMs that collect the light from POLAR target. Each scaler is incremented if at least one energy deposition greater than 50 keV has occured in the corresponding MAPM. When accumulating the scaler output for all photons or other background energy deposition produced during a GRB one obtains 25 numbers corresponding roughly to the number of photons above the 50 keV threshold. The counting pattern is sensitive to the direction of incoming photons since the size of the target corresponds to several absorption lengths. GEANT4 simulations demonstrate that the relative output of those scalers, accumulated over the duration of a GRB, can be used to determine the source position above POLAR.

## III. GRB Localization Method

Using the POLAR simulation package we created a database containing the scalers output, normalized to their number of entries, produced by very strong non-polarized GRBs located at numerous positions in the sky (figure 2 shows two normalized scaler outputs extracted from the database). The database consists of a grid of 10201 nodes that represent the same amount of GRB locations, uniformly distributed in the sky. The analysis has been performed in Cartesian coordinates to avoid numerical problems related to the indetermination of $\phi_\gamma$ close to the zenith:

$$\begin{aligned} x &= (1-\cos\theta_\gamma)\cdot\cos\phi_\gamma \\ y &= (1-\cos\theta_\gamma)\cdot\sin\phi_\gamma \end{aligned} \tag{2}$$

where $\theta_\gamma$ and $\phi_\gamma$ are the polar and azimuthal incoming angles from the GRB photons. The selection of this coordinate system guarantees a uniform grid where all points are equally distant from each other and the center of the coordinate system corresponds to the zenith of the detector.

When a GRB is observed, the output of the scaler is recorded and compared with the database by calculating the Pearson $\chi^2$ at each point of the grid (see figure 3). The minimum of this 2-dimensional $\chi^2$ distribution is found by fitting two parabolas, in the $x$ and $y$ directions, around the lowest node of the grid. The minimum of those parabolas gives the value of the coordinates where the GRB was located. The error associated to the found location is calculated from the points where the

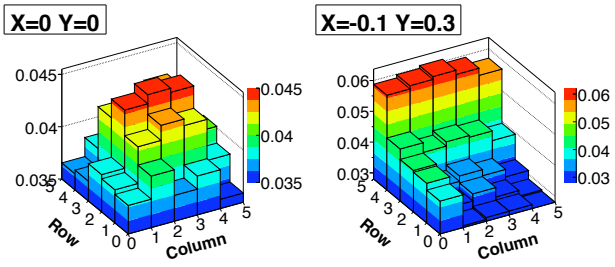


Fig. 2: Graphical representation of two of the normalized scaler output (NSO) patterns that constitute the database.

parabolas take the values $\chi^2_{min}(x)+1$ and $\chi^2_{min}(y)+1$, respectively.

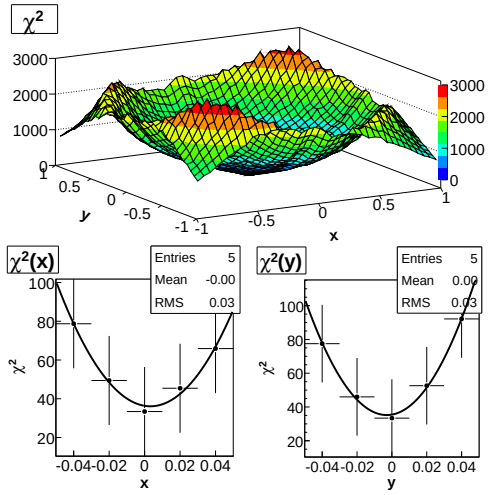


Fig. 3: Example of $\chi^2$ minimization. The distribution of $\chi^2$ in the ($x$,$y$) plane is shown in the top, and the parabolic fits of both variables in the bottom. The measurement used in this example was produced using the POLAR simulation package with a non-polarized GRB of $F_{tot} = 10^{-5}$ erg cm$^{-2}$, $\alpha$=-1.0, $\beta$=-2.5, $E_{peak}$=200 keV located at POLAR zenith.

We have performed several series of simulations to estimate the capabilities of the GRB localization method and the influence of its uncertainty into the measured level of polarization. When simulating strong non-polarized GRBs (see figure 4) with a total fluence $F_{tot} = 10^{-5}$ erg cm$^{-2}$ and a similar spectral shape to the ones used to create the database, the position coordinates could be determined with a maximal error of 0.07 (equivalent to being able to determine the position in spherical coordinates ($\theta_\gamma$, $\phi_\gamma$) with a maximal error of $\sim 5^\circ$ for $\theta_\gamma > 30^\circ$).

When a GRB is detected by POLAR its level of polarization ($\Pi$) is determined from the amplitude ($\mu$) of the modulation curve and the 100% modulation factor ($\mu_{100}$) using: $\Pi = \mu/\mu_{100}$. Since $\mu_{100}$ varies with the burst position and spectral shape, $\Pi$ must be calculated using a $\mu_{100}$ derived from simulations of a GRB with the same spectrum and position in the sky as the observed

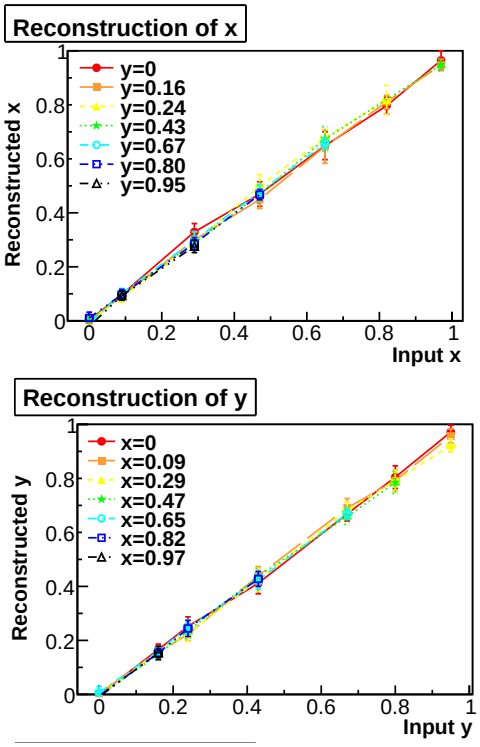


Fig. 4: Results from simulated non-polarized strong GRBs ($F_{tot} = 10^{-5}$ erg cm$^{-2}$). *Top*: Linearity plot in $x$, i.e. reconstructed $x$ vs. input $x$ for several fixed $y$ values. Each point on this graph represents the average of the 10 simulations made at each position. Its error bar corresponds to the standard deviation of the 10 measurements performed. *Bottom*: Equivalent to the plot on the top, but calculated for $y$ at several fixed $x$ positions. In both plots lines of different styles have been drawn to guide the eye.

one. When the location of the GRB is unknown, the value of $\mu_{100}$ needed to calculate $\Pi$ is also unknown. Therefore the uncertainty on the position of the GRB is translated to an uncertainty in the value of $\mu_{100}$ and further into an error on the resultant level of polarization. With the values of position uncertainty found from figure 4, the error in the $\mu_{100}$ of the measured GRB was found to be $\leq 6\%$ (see figure 5). Considering GRBs of similar strength but different spectral shapes, the coordinates could be determined with a maximal error of 0.14, keeping the error on $\mu_{100}$ below 10%. For weaker GRBs of fluence $F_{tot} \approx 10^{-6}$ erg cm$^{-2}$ the error in $\mu_{100}$ could be restricted only below about 20%.

There are several effects that could potentially modify the performance of the GRB localization technique. We have studied the most important ones: asymmetries produced by GRB polarization, diffuse $\gamma$-ray background, GRB spectral variations, satellite backscattering, fluctuations in light-collection efficiency, and MAPM non-uniform sensitivity. We found that the degree of polarization of the GRBs, the presence of a satellite behind POLAR, the fluctuations in

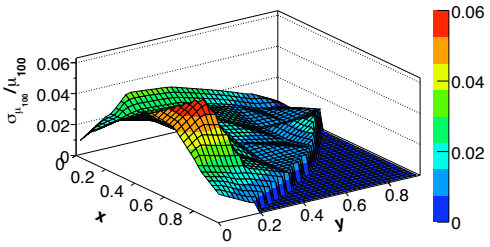


Fig. 5: Distribution of 100% modulation factor ($\mu_{100}$) vs. $x$ and $y$, calculated for a strong GRB of total fluence $\mathrm{F_{tot}} \approx 10^{-5}$ erg cm$^{-2}$ and same spectral shape as the database. To facilitate the visualization only one quadrant of the sky ($x > 0$ and $y > 0$) is shown. The empty area at the right of the image corresponds to positions where the GRB would be below POLAR. In such a situation the presence of the satellite is be a very important factor than would probably preventing us from measuring polarization. Therefore we did not consider this case in the analysis.

light-collection efficiency, and the MAPM non-uniform sensitivity do not modify the performance of the localization method. Regarding the diffuse $\gamma$-ray background, its spectrum was simulated according to the analytical expression presented in [16], but with a 10% increase in its absolute normalization factor, as suggested by [17]. It was found that in the case of strong short GRBs the diffuse $\gamma$-ray can be neglected, but for long GRBs the estimation must not differ from the real background level by more than 8%. When the background is not strongly variable, it is sufficient to average two background measurements one taken immediately before and the other immediately after the GRB. If the total time span measured outside the GRB is equal to the burst duration, one obtains the level of background with r.m.s. equal to ∼7% of its absolute value. Finally, it was seen that variations on the GRB spectral shape produced a strong bias in the reconstructed burst position when the scalers threshold was kept very low (5 keV). To mitigate the problem we raised the energy threshold of the scaler to 50 keV. In this way we largely reduce the sensitivity of the method to spectral variations, so that the error inflicted into $\mu_{100}$ due to the uncertainty in the localization method is below 10% for GRBs of a total fluence $\mathrm{F_{tot}} = 10^{-5}$ erg cm$^{-2}$.

| **Systematic Effect** | Impact |
|---|---|
| GRB polarization | None |
| Background (8% accuracy subtraction) | $\sigma_{\mu_{100}}/\mu_{100} < 10\%$ |
| Variations GRB spectral shape | $\sigma_{\mu_{100}}/\mu_{100} \leq 10\%$ |
| Satellite backscattering | None |
| Statistical fluctuations in light collection | None |
| Nonuniform sensitivity of MAPMs | None |

TABLE I: Impact of several systematic effects in the POLAR GRB localization method.

## IV. Conclusions

The GRB localization technique will provide enough accuracy to allow for the measurement of the GRBs polarization level with only a small increase on its error. For a GRB of total fluence $\mathrm{F_{tot}} = 10^{-5}$ erg cm$^{-2}$, the added error is negligible at low polarization levels, compared with the one from the measured modulation factor itself. At large polarization levels the error from the localization is larger than the one from the measured modulation factor, but all together reaching no more than 15% of the measured polarization.

The method here presented can be experimentally tested when flat and uniformly illuminating the complete POLAR target with a radioactive source to be placed at various locations. Such a kind of test will be performed when the POLAR engineering qualification model will be ready. In flight, if other instrument can provide the position of one or several GRBs detected by POLAR, a direct comparison with the output of the localization method can be done. In general, the precision in the localization provided by instruments with imaging capabilities will be better than that of POLAR alone, and preferred to it. The Interplanetary Network (IPN)[18] is able to localize GRBs with very good precision, and its extension in time is currently under discussion. The POLAR localization capability will be useful for those cases where no other instruments are simultaneously observing the same field of view.

## References

[1] D. Band, J. Matteson, L. Ford, et al., ApJ. 413 (1993) 281.
[2] D. Lazzati, New Journal of Physics Vol 8, Issue 8 (2006) 131.
[3] K. Toma, T. Sakamoto, B. Zhang, et al., submitted ApJ, arXiv:0812.2483v1(2008).
[4] R. Marcinkowski, D. Haas, W. Hajdas, et al., ICRC2009 Conf. Proc., Abstract ID:38, (2005).
[5] N. Produit, F. Barao, S. Deluit, et al., Nucl. Instr. and Meth. A550 (2005) 616.
[6] P.F. Bloser, J.S. Legere, J.R. Macri, et al., Chin. J. Astron. Astroph. Suppl. Vol. 6 Issue S1 (2006) 393.
[7] J.E. Hill, M.L. McConnell, P. Bloser, et al., AIP Conf. Proc. 1065 (2008) 331.
[8] R,M. Curado da Silva, E. Caroli, J.B. Stephen, et al., Exp. Astron. Vol 15, Issue 1 (2003) 45.
[9] S. Gunji, H. Sakurai, F. Tokanai, et al., SPIE Conf. Proc 686 (2007) 668618.
[10] E. Costa, R. Bellazzini, G. Tagliaferri, et al., SPIE Conf. Proc. 6686 (2007) 6686Z.
[11] E. Costa, R. Bellazzini, P. Soffitta, et al., SPIE Conf. Proc. 6266 (2006) 62660R.
[12] M.L. McConnell, J.M. Ryan, D.M. Smith, et al., Solar Phys. 210 (2002) 125.
[13] F. Lei, A.J. Dean, and G.L. Hills, Space Sci. Rev. 82 (1997) 309.
[14] S. Agostinelli, J. Allison, K. Amako, et al., Nucl. Instrum. Meth. A 506 (2003) 250
[15] R. Brun, F. Rademakers, Nucl. Instr. and Meth. A Vol 389, Issues 1-2 (1997) 81
[16] D.E. Gruber, J.L. Matteson, L.E. Peterson, et al., ApJ 520 (1999) 124.
[17] E. Churazov, R. Sunyaev, M. Revninvtsev, et al. A&A 467 2 (2007) 529.
[18] K. Hurley, Paper number: E18-0039-08, 7th COSPAR Scientific Assembly, Montréal, Canada (2008)